Transitional Properties of Cotton Fibers from Cellulose I to Cellulose II Structure

Yiying Yue,[a,b] Guangping Han,[a,*] and Qinglin Wu [b,*]

Mercerized fibers were prepared from native cotton fabrics via NaOH solution treatment at different concentrations. Mercerization led to transformation of the crystal structure of cotton fibers from cellulose I to II when the NaOH concentration was greater than 10 wt%. In addition, the cotton fibers were converted into a swollen and rough state after mercerization treatment. The results of Fourier transform infrared spectrometry and wide-angle X-ray diffraction indicated that the cellulose molecular structure changed (*e.g.* the degree of disorder of O-H stretching vibration increased, while the crystallinity index decreased) in the process of mercerization. Thermogravimetric analysis determined that the cellulose II fibers were more thermally stable than the cellulose I fibers. The mechanical properties of cellulose fiber-reinforced polyethylene oxide (PEO) composites showed that both original and mercerized cotton fibers enhanced the tensile strength of the PEO matrix. These properties directly contributed to the advantages of mercerized textile products (*e.g*. higher luster, holds more dye, more effectively absorbs perspiration, and tougher under different washing conditions).

Keywords: Cotton fiber; Cellulose I; Cellulose II; Mercerization; Properties

Contact information: a: Key Laboratory of Bio-based Material Science and Technology (Ministry of Education), Northeast Forestry University, Harbin 150040, China; b: School of Renewable Natural Resources, Louisiana State University Agricultural Center, Baton Rouge, LA 70803, USA;
** Corresponding authors: guangpingh@hotmail.com; wuqing@lsu.edu*

INTRODUCTION

Cellulose, which is one of the most promising renewable polymeric materials on earth, exhibits fascinating structures and properties. It consists of β-1,-4- linked chains of D-glucose, where the glucose units are in 6-membered rings (*i.e*., pyranoses) joined by single oxygen atoms (acetal linkages) between the C-1 of one pyranose ring and the C-4 of the next ring (Nishimura *et al*. 1991). The crystal structure of native cellulose can be converted to that of cellulose II by NaOH treatment, known as mercerization. It has been reported that the cellulose I structure is made of parallel chains characterized by an intermolecular hydrogen bond network extending from the O_2-H hydroxyl to the O_6 ring oxygen of the next unit (Nishiyama *et al*. 2008). While the crystal structure of cellulose II is described as anti-parallel, stabilized by an intermolecular hydrogen bond network of O_2-H---O_6, O_6-H---O_6, and O_2-H---O_2 (Langan *et al*. 1999).

Mercerization treatment of natural cellulose fibers results in a structural transformation from cellulose I to II. During the process, the form of the crystalline lattice is changed because of the transformation of hydroxymethyl and the polarity of the chains (Oh *et al*. 2005). However, its fibrous structure is largely kept intact. The mercerization process also affects the twisting and swelling of cellulose fibers. This is because Na^+ ions play a crucial role in widening the accessible regions between the

lattice planes to allow the ions to diffuse into those planes (Gwon *et al*. 2010). During mercerization, cellulose I proceeds through a crystal-to-crystal phase transformation. The intermediate structure between the parallel chain structure of cellulose I and the anti-parallel chain structure of cellulose II is Na-cellulose I (Gwon *et al*. 2010; Mansikkamaki *et al*. 2005). Na-cellulose I is developed in the amorphous region of cellulose, and there is a relatively large distance between cellulose molecules because OH groups in the cellulose fiber are changed into O-Na groups. After a rinsing process, Na+ ions are removed by water, and a new crystalline structure, cellulose II, is achieved. The mechanism of mercerization has been widely studied; however, the transitional fiber properties need to be further discussed.

Changsarn *et al*. (2011) studied cellulose nanowhiskers based on polyethylene oxide (PEO) by electrospinning. A significant enhancement of PEO latex upon incorporating small amounts of nanowhiskers was reported. The interaction of cellulose nanocrystals and nanofibrils with PEO matrix and the resulted reinforcing effects on the matrix polymer were also reported (Xu *et al.* 2013). The results showed that both PEO/ nanofibrils and PEO/nanocrystals composites achieved very high young's modulus. The bacteria cellulose nanofibers were acetylated to enhance the properties of optically transparent composites of acrylic resin reinforced with the nanofibers (Ifuku *et al*. 2007). Liu *et al.* (2010) reported the improved mechanical properties of polymethylmethacrylate film through the reinforcement from cellulose nanocrystals.

The present work investigated the effect of mercerization on the properties of cellulose fibers. The objective of this study was to characterize the morphology, functional groups, crystal structure, and thermal properties of cotton cellulose fibers as a function of mercerization treatment and to study their application as reinforcement in a PEO matrix.

EXPERIMENTAL

Raw Materials and Processing

Cotton fabrics were provided by the USDA ARS Southern Regional Research Center in New Orleans, LA. The fabric sample was first cut into 5 × 25-mm pieces using a fabric cutter, then further processed with a Wiley mill (Arthur H. Thomas Co.) to pass a 100-mesh screen. The obtained cotton particles were randomly divided into two parts and then stored in two separate bags for further processing.

Mercerization Treatment

Mercerization was conducted with one of the two bags of the pre-prepared cotton fibers. About 30 g of cotton fiber was subjected to NaOH solution treatment for 4 h at room temperature. Five NaOH concentrations were used, *i.e.*, 0, 5, 10, 15, and 20 wt%. The obtained slurry was filtered and thoroughly washed with distilled water until the wash water reached a neutral pH. The prepared fiber samples were then dried at 40 °C in a vacuum oven for 48 h prior to analysis of the effects of mercerization. The cotton samples obtained were designated Cx, where x = 0, 5, 10, 15, and 20 according to the concentration of alkaline solution. For instance, the sample with no alkali treatment was marked C0, and the sample treated with 5% alkali solution was C5.

Fabrication of Cotton Fiber-reinforced Composite Films

1 mg of cellulose I (C0) and cellulose II (C20) cotton fibers were added to 50 mL of 0.5 wt% PEO suspension (molecular mass 20,000 g/mol), respectively. The resulting mixture was intensely stirred to achieve a uniform dispersion of cellulose cotton fiber in the polymer matrix. Finally, 20 mL of the solution was cast in plastic dishes (inter diameter 87 mm) and then dried in refrigerator at 10 °C for overnight to obtain PEO/ cellulose I cotton fiber (C0), and PEO/cellulose II cotton fiber (C20) composite films.

Characterization

Morphological analysis

The morphology of cotton fibers was characterized using field emission scanning electron microscopy (FESEM, Nova^{TM} Nano SEM 450, Hillsboro, Oregon, USA). Prior to analysis, the raw and mercerized cotton fibers were coated with Au and then fixed on metal stubs using double-sided adhesive tape. The samples were scanned at 5 kV, and the images were recorded.

Fourier transform infrared (FTIR) spectrometry

The FTIR spectra of dry fiber samples were taken with a Bruker FTIR analyzer (Tensor-27, Bruker Optics Inc., Billerica, MA) using the attenuated total reflectance (ATR) mode. The data were recorded in the range of 4000 to 600 cm^{-1}. Each of the samples from various treatment conditions was pressed into the sample chamber for FTIR measurements. For each condition, three replicate measurements were made.

Wide-angle X-ray diffraction (WXRD)

The super-molecular structure of the native and mercerized cotton fibers was analyzed using a Bruker/Siemens D5000 automated wide-angle powder X-ray diffractometer. The X-ray diffraction pattern was recorded within an angle range of 0 to 40°. The wavelength of the Cu/Ka radiation source was 0.154 nm, and the spectra were obtained at 30 mA with an accelerating voltage of 40 kV. X-ray diffraction data were analyzed using the MDI Jade 5.0 software. Curve fitting was performed to find individual peak regions. The main diffraction peaks were integrated and used to calculate the crystalline index (CI, %) of the samples, as shown in Equation 1,

$$CI\ (\%) = \frac{I_c}{I_c + I_a} \times 100\ \% \quad (1)$$

where I_c and I_a represent the integrated intensities of the crystalline and amorphous regions, respectively.

The Scherrer equation was used to calculate the crystal size, t (nm), which was determined perpendicular to the (200) planes for both cellulose I and cellulose II samples,

$$t = \frac{K\ \lambda}{\beta\ Cos\ \theta} \quad (2)$$

where K is the correction factor and usually taken to be 0.9; λ is the radiation wavelength; θ is the diffraction angle; and β is the corrected angular width at half maximum intensity in radians.

The spacing between the (200) planes, d (nm), was calculated using Bragg's equation,

$$n\lambda = 2d \sin \theta \quad (3)$$

where n is an integer; λ is the wavelength of incident wave; and θ is the angle between the incident ray and the scattering plane.

Thermal analysis

The dehydration and degradation behavior of cotton fiber samples was characterized using a thermogravimetric analyzer (Q50, TA Instruments, New Castle, DE) in a nitrogen atmosphere. Specimens of 5 to 10 mg were tested in a temperature range of 30 to 500 °C. The heating rate was 5 °C/min, and the nitrogen flow rate was 65 mL/min. The weight loss rate was obtained from derivative thermogravimetric (DTG) data. The onset degradation temperature was defined as the intersection temperature of tangents drawn from a thermogravimetric curve, one before inflection caused by the degradation and another from the cellulose degradation step.

RESULTS AND DISCUSSION

Morphological Properties

Figures 1a and 1b show the FESEM images of native cotton fibers (C0) and mercerized cotton fibers (C20) at 2000× magnification, respectively. The insert in each figure shows an enlarged area at 10000× magnification. As shown in Fig. 1a, native cotton fibers had a relatively smooth surface, with a twisted, ribbon-like shape. The smooth surface was primarily due to a wax coating on the fiber surface. After mercerization (Fig. 1b), the fibers were converted into a swollen and roughened state, indicating that the assembly and orientation of microfibrils was completely disrupted. The rough surface of mercerized cotton fibers was a direct result of the surface wax layer being removed by alkali treatment.

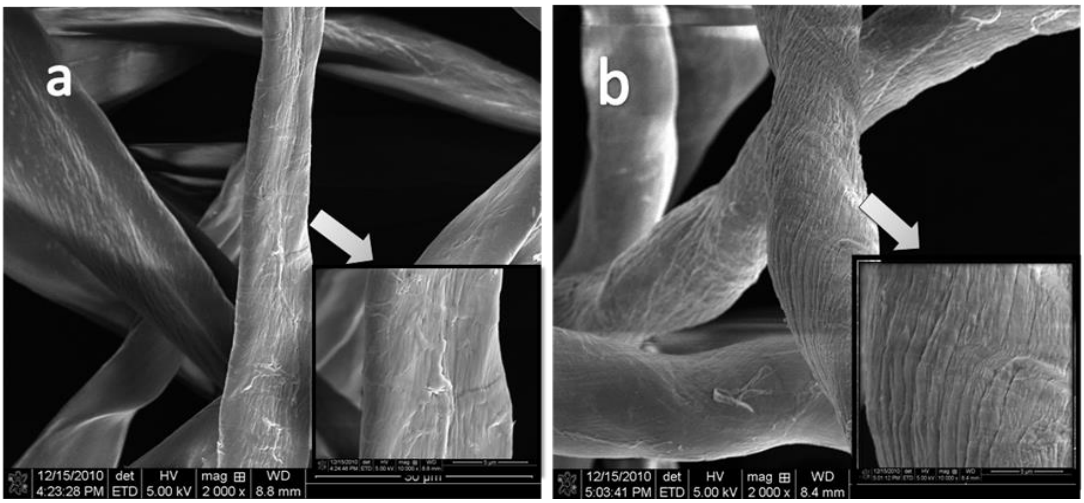

Fig. 1. FESEM images of native cotton (a) and mercerized cotton (b) fibers

A roughened fiber surface allows fibers to take dyes more easily and may also provide better interfacial bonding for fiber-polymer composite systems. Also, the surface of the of the nearly cylindrical cotton fiber after mercerization reflected light more evenly to all sides than the ribbon shaped cotton fiber and the fiber surface became more lustrous.

FTIR Characteristics

The FTIR characteristics of native and mercerized cotton fibers in the range of 4000 to 1000 cm^{-1} are shown in Fig. 2. As previously reported, bands located at 4000 to 2995 cm^{-1}, 2900 cm^{-1}, 1430 cm^{-1}, 1375 cm^{-1}, and 900 cm^{-1} were sensitive to variations in the crystalline and amorphous regions (Oh *et al*. 2005).

Figure 3 shows the replots of the FTIR spectra over selected regions to contrast the differences among various fibers. A strong hydrogen-bonded OH stretching vibration was observed in the region of 3600 to 2995 cm^{-1} (Fig. 3a). The intermolecular hydrogen bonding of O_2-H---O_6 for native fibers and O_2-H---O_6, O_6-H---O_6, and O_2-H---O_2 for mercerized fibers (Langan *et al.* 1999) are shown at 3438 cm^{-1}, 3334 cm^{-1}, and 3293 cm^{-1}, respectively (Oh *et al*. 2005; Schwanninger *et al*. 2004). It was shown that the crystal system of cellulose was changed from cellulose I to cellulose II at 15% and 20% alkali levels. The IR index (*i.e.*, the ratio of IR intensity at a given wavenumber to that at the reference wavenumber) values based on the absorbance peaks at 1054 cm^{-1} (>CO/C-C stretching vibration) were chosen to analyze the conformation and hydrogen bond intensity changes during the treatment (Das and Chakraborty 2006). The OH stretching vibration within the region of 3100 to 3800 cm^{-1} increased with an increase in the alkali concentration level. The IR index values for C0, C5, C10, C15, and C20 samples at 3334 cm^{-1} were calculated to be 0.286, 0.237, 0.233, 0.302, and 0.324, respectively. The results indicated that sodium hydroxide treatment intensified the intra- or inter-molecular hydrogen bonding. The degree of disorder of O-H stretching vibration increased the hygroscopic characteristics and made the fiber more effectively to absorb perspiration.

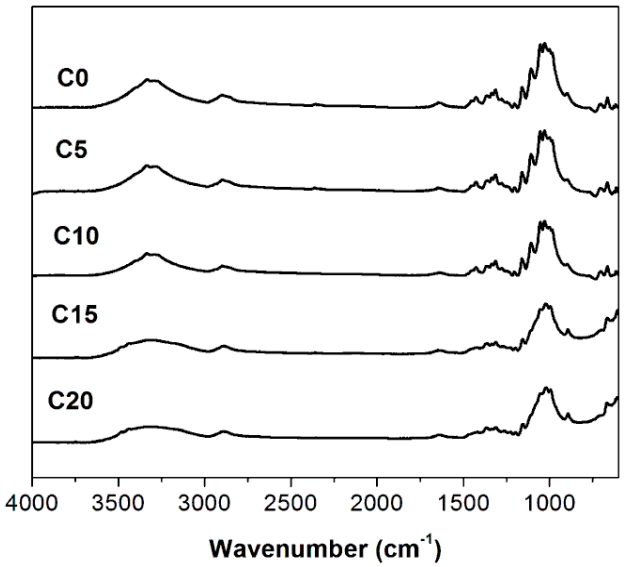

Fig. 2. The overall FTIR spectra of cotton fibers from C0, C5, C10, C15, and C20 samples

The maximum absorbance of -CH stretching vibration also shifted from about 2901 cm^{-1} for C0, C5, and C10 to a lower wavenumber at 2890 cm^{-1} for C15 and C20 after mercerization treatment (Fig. 3a). This transformation could be due to small changes in the torsion angles of the β-glycosidic linkages (Liu *et al*. 2010). The absorbance intensities at 1427 cm^{-1} were assigned to CH_2 bending (El-Wakil and Hassan 2008). The intensities of the peaks at 1427 cm^{-1} for C0, C5, C10, C15, and C20 cotton fibers were 0.144, 0.128, 0.133, 0.108, and 0.119, respectively (Fig. 3b).

The decreased CH_2 intensity bending reflected a higher number of disordered cotton structures formed with increasing sodium hydroxide concentration (Krebs 2008). The small change at 1370 cm^{-1} was attributed to the differing CO stretching vibrations in cellulose I and cellulose II fibers (Oh *et al.* 2005).

An important feature of the spectra shown in Fig. 3c was that the peaks of C15 and C20 shifted from 1160 cm^{-1} to 1156 cm^{-1}, indicating that the cellulose crystal structure switched from I to II. In addition, the decreased intensities of C15 and C20 suggested that the C-O-C stretching vibration bonding was changed at higher alkali levels.

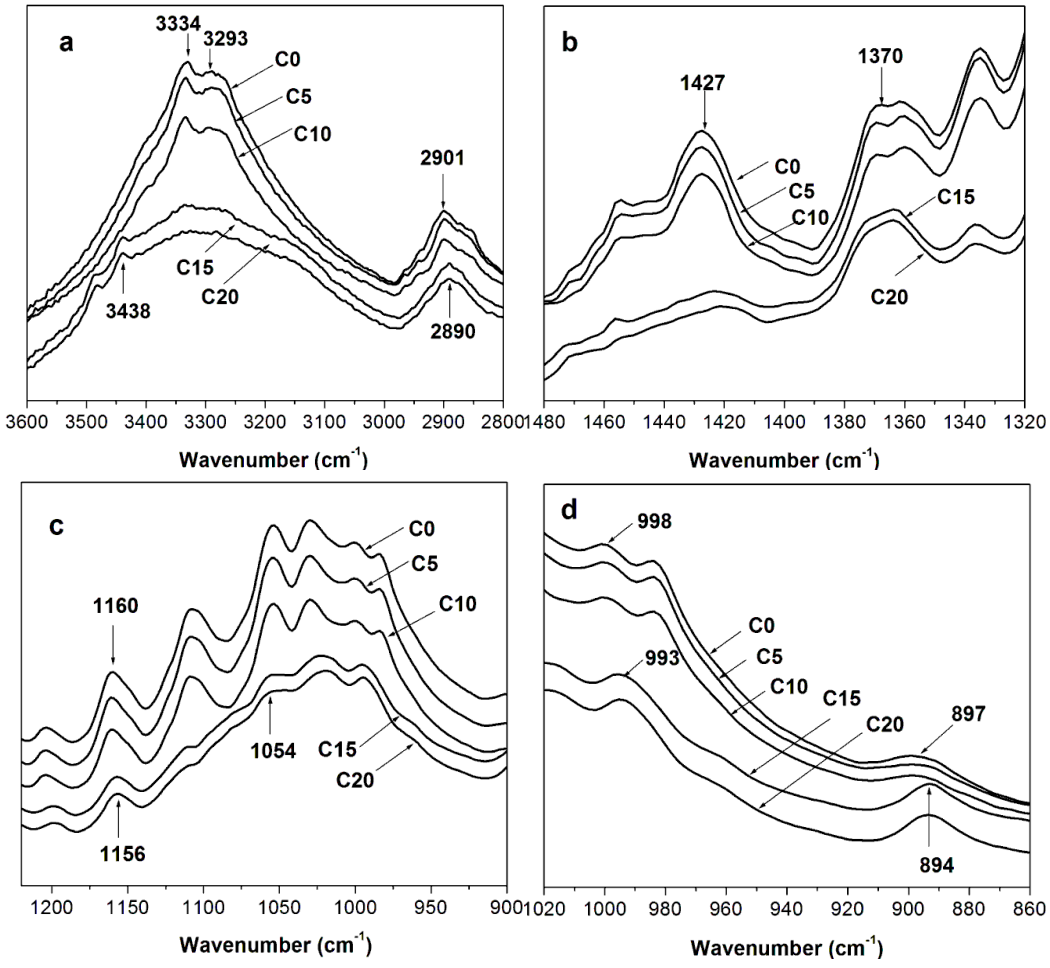

Fig. 3. FTIR spectra of the C0, C5, C10, C15, and C20 cotton fibers with the wavenumber ranges of 3600 to 2750 (a), 1480 to 1320 (b), 950 to 640 (c), and 1225 to 900 (d)

Figure 3d shows that the bands at 897 cm^{-1} shifted to 894 cm^{-1}. It was reported that the 897 cm^{-1} wavenumber can be assigned to the β-glucosidic linkage for the cellulose I structure and the 894 cm^{-1} wavenumber to the cellulose II structure (Gwon *et al.* 2010). This change was due to the rotation of glucose residue around the glucosidic bond (Ray and Sarkar 2001). The bands at 998 cm^{-1} shifted to 993 cm^{-1}, indicating the crystal structure transformation from cellulose I to II (Gwon et al. 2010).

WXRD Properties

The WXRD results showed that mercerization resulted in significant changes in the crystalline structure and crystallinity (Fig. 4). The diffraction pattern of native cotton (C0) and the fibers treated at 10% alkali concentration (C10) had three characteristic peaks of cellulose I crystal structure at 2θ = 14.62° ($1\bar{1}0$), 16.29° (110), and 22.48° (200) (Liu and Hu 2008). As the concentration of alkali increased, a significant variation in the diffraction pattern was observed. The crystalline peak was split into two weaker peaks located at 2θ = 20.1 (110) and 2θ = 21.53 (200) for C15 and C20 fibers, indicating the formation of cellulose II structure.

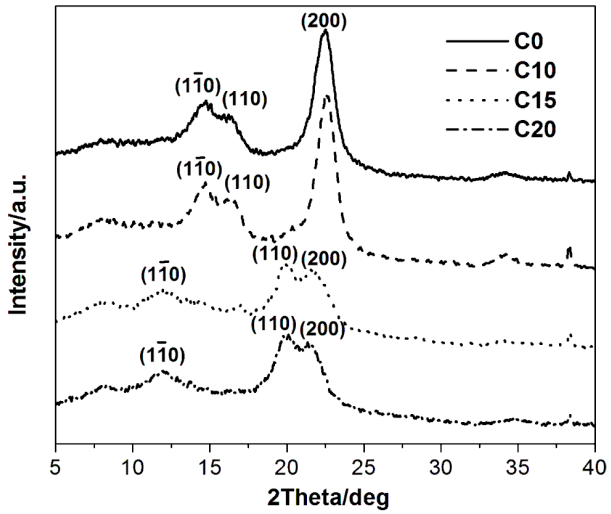

Fig. 4. X-ray diffraction analysis of native cotton and mercerized cotton fibers

Table 1. Crystallinity Parameters of Cotton Fibers Before and After Mercerization

Sample No.	Crystallinity index (%)	d-spacing (200) of the planes (nm)	Crystal size perpendicular to the (200) planes (nm)
C0	81.2	0.394	9.12
C10	83.0	0.394	9.27
C15	64.7	0.412	11.75
C20	66.5	0.415	11.05

The crystallinity parameters before and after mercerization are listed in Table 1. The crystallinity index (CI) is related to the strength and stiffness of fibers (Wang *et al*. 2007). The CI values for C0, C10, C15, and C20 were 81.2%, 83.0%, 64.7%, and 66.5%, respectively. There was a significant decrease in CI values for the C15 and C20 samples. Similar decreases in CI values for reconstituted cellulose II have been previously reported (Azubuike *et al*. 2012; Han *et al*. 2013a). Three distinct processes are known to occur

during mercerization: microfibril swelling, crystalline area disruption, and new crystalline lattice formation. Mercerization occurs only when the NaOH hydrates penetrate into the cellulose crystals to disrupt them and form new crystals, creating a new physical network in the swollen state. The NaOH hydrates need to be small enough to penetrate into the regions of higher lateral order (Lee *et al.* 2004). The size of the NaOH hydrates is known to decrease with increased alkali concentration. At lower NaOH concentrations (*i.e.*, C10), NaOH hydrates were too big to penetrate into the cellulose crystals to disrupt them. As a result, the CI value for the C10 sample showed little change. The crystalline structure of the cotton fibers was converted into a swollen state as the NaOH concentration was further increased. When the cellulose structure was in its most swollen state, it became easier for the hydrated hydroxide ions to penetrate the internal crystals and thoroughly react with the fiber, leading to a reduced CI value. However, the rate of penetration of the hydroxide ions became slower due to the increased viscosity of the NaOH solution at higher concentration levels (*e.g.*, 20%) (Okano and Sarko 1984; Okano and Sarko 1985). Thus, a NaOH concentration of approximately 15% was probably the most suitable for crystal lattice transformation and degradation of cotton fibers at the given temperature level. It should be noted that the conversion process of cellulose I to cellulose II also depended on the temperature of NaOH and the fiber mixture.

The results in Table 1 show that the inter-planar spacing between adjacent lattices for native cellulose fibers was 0.394 nm. However, the spacing became larger for cellulose II fibers (C15 and C20). Changes of crystal size in the (200) planes showed a similar tendency. The crystal sizes for cotton fibers varied from 9.12 nm to 11.75 nm. The results indicated that mercerized cellulose increased in crystal size and d-spacing. Mercerization resulted in the agglomeration of the β-1, 4-D-linked glucose chain or arrangement of strong intermolecular hydrogen bonds through the conversion of cellulose I to cellulose II.

Thermal Degradation Properties

Figure 5 shows TG (a) and DTG (b) curves of the native and mercerized cotton fibers. All samples had a small weight loss in the low temperature range (less than 110 °C), corresponding to the evaporation of absorbed water. In the high temperature range, all samples showed a similar one-step pyrolysis process with typical decomposition behavior.

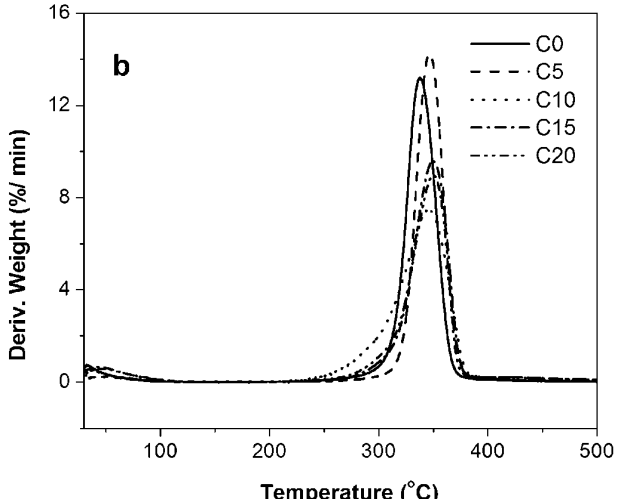

Fig. 5. TGA and DTG curves of native and mercerized cotton fibers

Table 2. TGA Parameters of Cotton Fibers Before and After Mercerization

Sample No.	Onset temp. T_o (°C)	Degradation temp. T_{max} (°C)	Maximum weight loss rate (%.min^{-1})	Char yield (wt%)
C0	316.82	332.70	13.10	6.48
C5	324.39	344.35	14.31	8.02
C10	310.71	342.50	7.59	10.34
C15	323.07	345.71	9.82	12.28
C20	320.89	345.32	8.95	15.49

Table 2 lists the onset temperature (T_o, °C), the maximum thermal degradation temperature (T_{max}, °C), the maximum weight loss rate, and the char yield for various samples. T_o and T_{max} varied significantly among the fibers with and without treatment. For the native cotton fibers, T_o occurred at 316.8 °C, with T_{max} at 332.7 °C. The degradation behavior of mercerized fibers was different. The onset temperatures for C5, C10, C15, and C20 were 324.39, 310.71, 323.07, and 329.89 °C, respectively. It was reported that the TG characteristics were closely correlated to the changes in crystallinity as a function of alkalization (Liu and Hu 2008).

The different thermal behaviors before and after mercerization were related to the change in cellulose structure. The increase in T_o for sample C5 was due to fibril swelling. The sharp decrease in T_o from C5 to C10 was probably due to partial destruction of the amorphous region. As the alkali concentration increased, the fibers went through a rearranging process to form a new crystalline lattice.

It can be seen from Table 2 that the degradation temperature and the mass loss rate followed the same trend. The char yield of the original cotton fibers was 6.48%. After mercerization, the char yield for C5, C10, C15, and C20 was 8.02, 10.34, 12.28, and 15.39%, respectively. This dramatic increase in char yield reflects the level of β-glycosidic linkages. Thus, mercerized cellulose with a stable structure exhibited an increase in char formation (Abbott and Bismarck 2010), indicating cellulose II cotton fibers were tougher under different washing conditions.

Properties of Cotton Fiber-reinforced Composite Films

Typical tensile strength and stress-strain curves for PEO, PEO/cellulose I cotton fiber (C0), and PEO/cellulose II cotton fiber (C20) composite films are shown in Fig. 6. The resulted thickness of all films averaged 60 μm. It was observed that both native and mercerized cotton fibers enhanced the PEO matrix.

Compared to the PEO/cellulose II cotton fiber composite (C20), the tensile strength and elongation at break for the PEO/cellulose I cotton fiber (C0) composite was slightly higher. This could be related to the fact that the mercerized cellulose fibers possessed more –OH groups on their surfaces, which may lead to a stronger interaction between the fibers and polymer matrix. However, it is also noted that the size and aspect ratio of cellulose II were smaller than those of cellulose I, resulting in a less entanglement of cellulose II fibers (Han *et al*. 2013b).

This result showed that the physical entanglement could significantly enhance the mechanical properties of PEO/cellulose I cotton fiber composite, while the cellulose II-reinforced PEO composite did not show a significant increase in mechanical properties due to the lack of tangling chains.

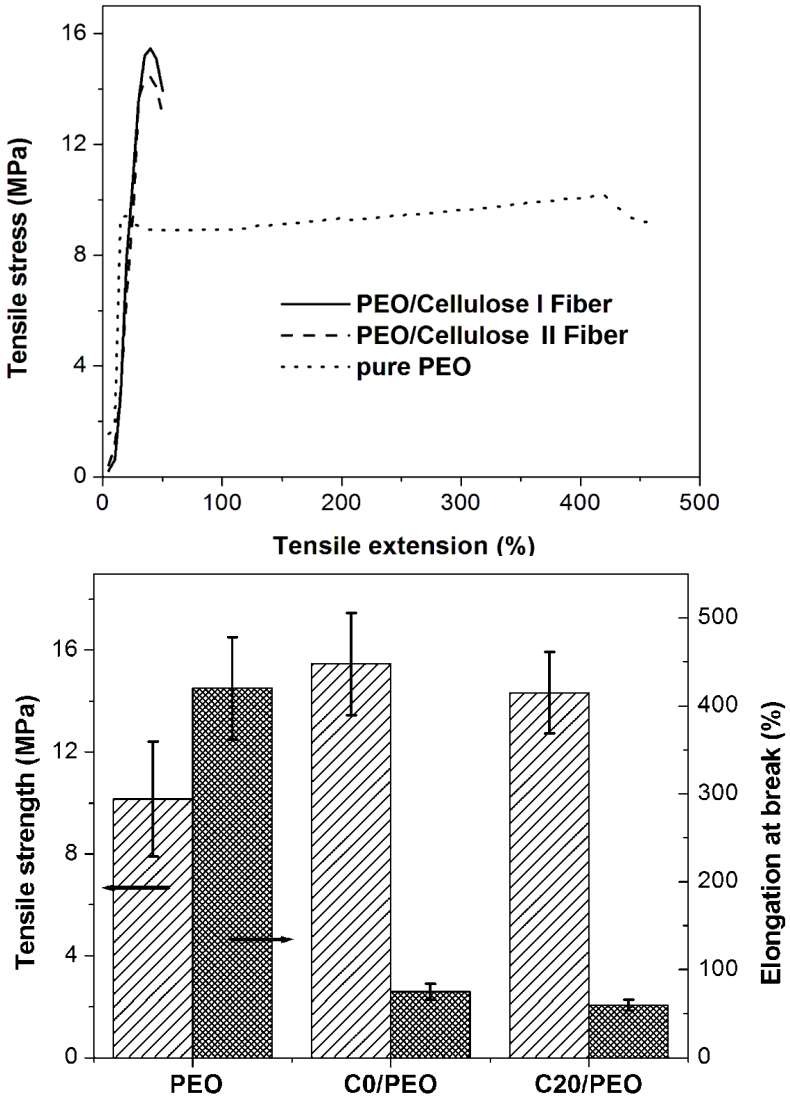

Fig. 6. Comparison of tensile strength of PEO, native, and mercerized fiber/PEO composite films

CONCLUSIONS

1. Mercerization of cotton fibers led to a crystal structural transformation from cellulose I to II. A complete transition occurred at sodium hydroxide concentration levels of 15 and 20 wt%.
2. Morphological observations revealed that the native cotton fibers had a relatively smooth surface with a twisted, ribbon-like shape. The fibers were converted into a swollen and roughened state by the mercerization treatment. The roughened fiber surfaces allowed fibers to take dyes more easily and the nearly cylindrical surface could reflect light more evenly to all sides, making fiber surface more lustrous.
3. FTIR and WXRD results indicated that the cellulose molecular structure changed in the process of mercerization. The degree of disorder of O-H stretching vibration

increased the hygroscopic characteristics and made the fiber more effective for the absorption of perspiration.

4. TGA analysis determined that the structure of cellulose II cotton fiber was more thermally stable than that of cellulose I fiber, resulting in the tougher cellulose II cotton fibers under different washing conditions.
5. The mechanical properties of fiber-reinforced PEO composites suggested that both raw and mercerized cotton fibers enhanced the tensile strength of the PEO matrix. The tensile strength and elongation at break for the PEO/cellulose I (C0) and PEO/cellulose II cotton fiber (C20) composites were almost the same, indicating that the effects of physical entanglement in C0 is as significant as chemical O-H group interaction in C20. Future study is needed to prove the stronger chemical interactions among mercerized cotton fibers than native cotton fibers.

ACKNOWLEDGMENTS

The financial support from the State Forestry Administration 948 project (Grant No. 2013-4-11), the National Natural Science Foundation (Grant No. 31070505), and the USDA CSREES (Grant Number: 2008-38814-04771) are highly appreciated.

REFERENCES CITED

Abbott, A., and Bismarck, A. (2010). "Self-reinforced cellulose nanocomposites," *Cellulose* 17(4), 779-791.

Azubuike, C. P., Rodriguez, H., Okhamafe, A. O., and Rogers, R. D. (2012). "Physicochemical properties of maize cob cellulose powders reconstituted from ionic liquid solution," *Cellulose* 19(2), 425-433.

Changsarn, S., Mendez, J. D., Shanmuganathan, K., Foster, E. J., Weder, C., and Supaphol, P. (2011). "Biologically inspired hierarchical design of nanocomposites based on poly(ethylene oxide) and cellulose nanofibers," *Macromolecular Rapid Communications* 32, 1367-1372.

El-Wakil, N. A., and Hassan, M. L. (2008). "Structural changes of regenerated cellulose dissolved in FeTNa, NaOH/thiourea, and NMMO systems," *J. Appl. Polym. Sci.* 109(5), 2862-2871.

Gwon, J. G., Lee, S. Y., Doh, G. H., and Kim, J. H. (2010). "Characterization of chemically modified wood fibers using FTIR spectroscopy for biocomposites," *J. Appl. Polym. Sci.* 116(6), 3212-3219.

Han, J, Zhou C, French AD, Han G, Wu Q. (2013a). "Characterization of cellulose II nanoparticles regenerated from 1-butyl-3-methylimidazolium chloride," *Carbohydr. Polym.* 94(2), 773-781.

Han, J, Zhou C, Wu Y, Liu F, Wu Q. (2013b). "Self-assembling behavior of cellulose nanoparticles during freeze-drying: Effect of suspension concentration, particle size, crystal structure, and surface charge," *Biomacromolecules* 14(5),1529-1540.

Ifuku, S., Nogi, M., Abe, K., Handa, K., Nakatsubo, F., and Yano, H. (2007). "Surface modification of bacterial cellulose nanofibers for property enhancement of optically transparent composites: Dependence on acetyl-group DS," *Biomacromolecules* 8,

1973-1978.
Krebs, F. C. (2008). "Degradation and stability of polymer and organic solar cells," *Sol. Energ. Mat. Sol. Cells* 92(7), 685.
Langan, P., Nishiyama, Y., and Chanzy, H. (1999). "A revised structure and hydrogen-bonding system in cellulose II from a neutron fiber diffraction analysis," *J. Am. Chem. Soc.* 121(43), 9940-9946.
Liu, H. Y., Liu, D. G., Yao, F., and Wu, Q. (2010). "Fabrication and properties of transparent polymethylmethacrylate/cellulose nanocrystals composites," *Bioresource Technology* 101, 5685-5692.
Liu, X. X., Khor, S., Petinakis, E., Yu, L., Simon, G., Dean, K., and Bateman, S. (2010). "Effects of hydrophilic fillers on the thermal degradation of poly(lactic acid)," *Thermochim. Acta* 509(1-2), 147-151.
Liu, Y. P., and Hu, H. (2008). "X-ray diffraction study of bamboo fibers treated with NaOH," *Fiber Polym.* 9(6), 735-739.
Lee, M. H., Park, H. S., Yoon, K. J., and Hauser, P. J. (2004). "Enhancing the durability of linen-like properties of low temperature mercerized cotton," *Text. Res. J.* 74(2), 146-154.
Mansikkamaki, P., Lahtinen, M., and Rissanen, K. (2005). "Structural changes of cellulose crystallites induced by mercerisation in different solvent systems determined by powder X-ray diffraction method," *Cellulose* 12(3), 233-242.
Nishimura, H., Okano, T., and Sarko, A. (1991). "Mercerization of cellulose .5. Crystal and molecular-structure of Na-cellulose I," *Macromolecules* 24(3), 759-770.
Nishiyama, Y., Johnson, G. P., French, A. D., Forsyth, V. T., and Langan, P. (2008). "Neutron crystallography, molecular dynamics, and quantum mechanics studies of the nature of hydrogen bonding in cellulose I-beta," *Biomacromolecules* 9(11), 3133-3140.
Oh, S. Y., Yoo, D. I., Shin, Y., and Seo, G. (2005). "FTIR analysis of cellulose treated with sodium hydroxide and carbon dioxide," *Carbohyd. Res.* 340(3), 417-428.
Okano, T., and Sarko, A. (1984). "Mercerization of cellulose .1. X-ray-diffraction evidence for intermediate structures," *J. Appl. Polym. Sci.* 29(12), 4175-4182.
Okano, T., and Sarko, A. (1985). "Mercerization of cellulose .2. Alkali cellulose intermediates and a possible mercerization mechanism," *J. Appl. Polym. Sci.* 30(1), 325-332.
Ray, D., and Sarkar, B. K. (2001). "Characterization of alkali-treated jute fibers for physical and mechanical properties," *J. Appl. Polym. Sci.* 80(7), 1013-1020.
Schwanninger, M., Rodrigues, J. C., Pereira, H., and Hinterstoisser, B. (2004). "Effects of short-time vibratory ball milling on the shape of FTIR spectra of cellulose," *Vib. Spectrosc.* 36(1), 23-40.
Wang, L. L., Han, G. T., and Zhang, Y. M. (2007). "Comparative study of composition, structure and properties of *Apocynum venetum* fibers under different pretreatments," *Carbohydrate Polymers* 69(2), 391-397.
Xu, X. Z., Liu, F., Jiang, L., Zhu, J. Y., Haagenson, D., and Wiesenborn, D. P. (2013). "Cellulose nanocrystals *vs*. cellulose nanofibrils: A comparative study on their microstructures and effects as polymer reinforcing agents," *ACS Applied Materials & Interfaces* 5, 2999-3009.

Article submitted: April 17, 2013; Peer review completed: May 27, 2013; Revision received: October 16, 2013; Accepted: October 17, 2013; Published: October 25, 2013.